

# Beamforming towards regions of interest for multi-site mobile networks

Paul Hurley\*, Matthieu Simeoni\*†

\*IBM Zurich Research Laboratory, CH-8803 Rüschlikon, Switzerland

†École Polytechnique Fédérale de Lausanne (EPFL), CH-1015 Lausanne, Switzerland

Email: pah@zurich.ibm.com, meo@zurich.ibm.com

**Abstract**—We show how a beamforming technique for analytical spatial filtering, called flexibeam, can be applied to mobile phone mast broadcasting so as to result in concentrations of power where most devices are.

To that end, flexibeam is interpreted as transmission beamforming. An analytically described radiation pattern is extended from a sphere to Euclidean space. A continuous beamforming function is then obtained by the Fourier transform of the extended radiation pattern. We then show how a Gaussian filter can be approximately achieved using beamforming.

The method is then expanded by means of an example of a collection of mobile phone masts covering an area of Zurich city so as to concentrate energy where devices are concentrated.

## I. INTRODUCTION

Beamforming has been deployed in mobile phone standards starting already with 2G. The techniques have become ever more sophisticated with each iteration. 4G/LTE, for example, deploys MIMO-based beamforming.

In general, direct multi-user beamforming [1], [2] – creating beams for each individual devices from mobile phone masts – is a gargantuan task. There are simply too many users, and a steady stream of accurate channel feedback [3] would be required to account people and vehicles moving around.

Yet algorithms deployed to date are variations on a theme within the MIMO framework: steering the beam towards a single point [4], [5], [6]. In practise, one would like to be able to concentrate energy in a way commensurate with the locations of devices, namely target areas of interest not single points, all the while building in tolerance for movement and imprecise location information.

To increase received power, LTE devices can receive signal from multiple base stations. This is a complex coordination protocol in general, and one key component to its efficiency is to have base stations target areas of importance. In this paper, we apply a technique called flexibeam, which determines beamforming weights that when applied approximate an optimal radiation pattern, so as to enable base stations to jointly concentrate energy where most devices are. The analytic framework allows tractable, numerically stable determination of beamforming weights. Aiming for areas rather than points minimises the required update rate, and reduces the communication requirement.

To this end, Section II derives flexibeam from an explicit transmit beamforming perspective. We then, in Section III, illustrate its application using a Gaussian approximation to

track an object in the presence of uncertainty. Afterwards, in Section III, we illustrate how energy can be concentrated around a certain area. There we take an example of devices concentrated around an area of Zurich city, and show how the target radiation pattern can be approximated by a series of Gaussian filters. We then illustrate how to determine each base station's beamforming weights so as to concentrate energy where most devices are.

## II. FLEXIBEAM FROM THE TRANSMIT PERSPECTIVE

In [7], we derived the receiving case for flexibeam. As a consequence of the reciprocity theorem [8], beam-shapes so designed can be used to receive or transmit. However, to gain insight into its operation and application, we now derive the transmission case directly.

Consider an array of  $L$  omni-directional receiving antennas, with unit gains and positions  $\mathbf{p}_1, \dots, \mathbf{p}_L \in \mathbb{R}^n$ . Each antenna emit an identical narrow-band signal  $s(t) \in \mathbb{C}$ . Without loss of generality, let the wavelength of this signal be  $\lambda = 1$ . The signals originating from each antenna will sum coherently, producing a radiation pattern, also called *beam-shape* of the antenna array. To control this radiation pattern, different delays and gains are introduced at each antenna:

$$x_i(t) = \gamma_i e^{j\phi_i} s(t), \quad (1)$$

where  $\gamma_i > 0$  and  $\phi_i \in [0, 2\pi]$  are respectively the gain and phase delay for antenna  $i$ . The signal seen at a *far field* target with position  $\mathbf{r} \in \mathbb{S}^{n-1}$  is given by [8], [9]

$$\begin{aligned} y(t, \mathbf{r}) &= s(t) \left( \sum_{i=1}^L \gamma_i e^{j\phi_i} e^{-j2\pi\langle \mathbf{r}, \mathbf{p}_i \rangle} \right), \\ &= s(t) \left( \sum_{i=1}^L w_i^* e^{-j2\pi\langle \mathbf{r}, \mathbf{p}_i \rangle} \right), \\ &= s(t) b^*(\mathbf{r}), \end{aligned} \quad (2)$$

where  $b(\mathbf{r}) = \sum_{i=1}^L w_i e^{j2\pi\langle \mathbf{r}, \mathbf{p}_i \rangle}$  is the array *beam-shape*, and  $w_i = \gamma_i e^{-j\phi_i} \in \mathbb{C}$  are the *beamforming weights*. We observe that beamforming is here the result of the physical summation of the signals emitted by each antenna.

For matched beamforming (cf. Fig. 1), the beamforming weights are chosen by

$$w_i = e^{-j2\pi\langle \mathbf{r}_0, \mathbf{p}_i \rangle}, \quad i = 1, \dots, L,$$

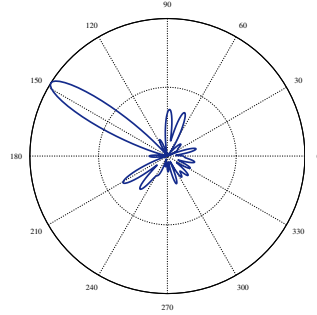


Fig. 1: Example beam-shape obtained with matched beamforming.

where  $\mathbf{r}_0 \in \mathbb{S}^{n-1}$  is the *steering direction*. Thus, the gains and delays at each antenna are respectively  $\gamma_i = 1$  and  $\phi_i = 2\pi\langle \mathbf{r}_0, \mathbf{p}_i \rangle$ .

Now consider a notional continuous field of antennas covering  $\mathbb{R}^n$ , over which we define a *broadcast function*  $x(t, \mathbf{p}) \in \mathcal{L}^2(\mathbb{R}^n, \mathbb{C})$ . This describes the signal that would be broadcasted by an antenna located at position  $\mathbf{p}$ , and extends (1) to cover all points in  $\mathbb{R}^n$ :

$$x(t, \mathbf{p}) = \gamma(\mathbf{p}) e^{j\phi(\mathbf{p})} s(t) = w^*(\mathbf{p}) s(t),$$

where  $w \in \mathcal{L}^2(\mathbb{R}^n, \mathbb{C})$  is the *beamforming function*, that generalises the concept of beamforming weights, and describes the gains and delays to be applied at each position  $\mathbf{p} \in \mathbb{R}^n$ . The signals emitted by this continuous field of antennas generate constructive interference, and Eq. (2) becomes

$$\begin{aligned} y(t, \mathbf{r}) &= s(t) \left( \int_{\mathbb{R}^n} w^*(\mathbf{p}) e^{-j2\pi\langle \mathbf{r}, \mathbf{p} \rangle} d\mathbf{p} \right), \\ &= s(t) \hat{w}^*(\mathbf{r}). \end{aligned} \quad (3)$$

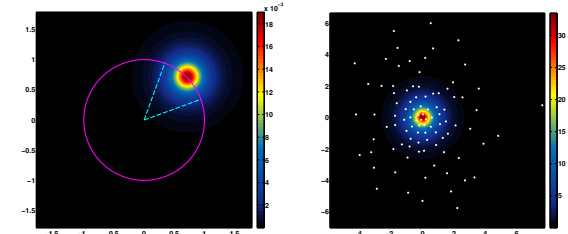
The beam-shape for the notional antenna field is then  $\hat{w}(\mathbf{r}) \in \mathcal{L}^2(\mathbb{S}^{n-1}, \mathbb{C})$ . It describes the radiation strength of the beamformed antenna field towards various directions, and as such acts as a spatial filter. The link to the beamforming function is as follows:

$$\hat{w}(\mathbf{r}) = \int_{\mathbb{R}^n} w(\mathbf{p}) e^{j2\pi\langle \mathbf{r}, \mathbf{p} \rangle} d\mathbf{p}.$$

The beamforming function was defined thus far only over the sphere  $\mathbb{S}^{n-1}$ . To enable sampling at any point in the plane, and to have a realisable  $n$ -dimensional Fourier transform relationship, the filter needs to be extended to  $\mathbb{R}^n$ . Let then  $\hat{\omega} : \mathbb{R}^n \rightarrow \mathbb{C}$  be a function whose  $n$ D Fourier transform exists, and on the hypersphere  $\mathbb{S}^{n-1}$  is equal to the target radiation pattern we would like to achieve. We call  $\hat{\omega}(\mathbf{r})$  thus designed the *extended radiation pattern*.

The actual choice of extension is application dependent, and part of the design. The beamforming function can now be computed by the Fourier transform

$$w(\mathbf{p}) = \int_{\mathbb{R}^n} \hat{w}(\mathbf{r}) e^{-j2\pi\langle \mathbf{r}, \mathbf{p} \rangle} d\mathbf{r}. \quad (4)$$



(a) Extended radiation pattern. Over the unit circle it approximates well the target radiation pattern.  
 (b) Magnitude of its 2D Fourier transform. The white dots denote the beamforming weights.

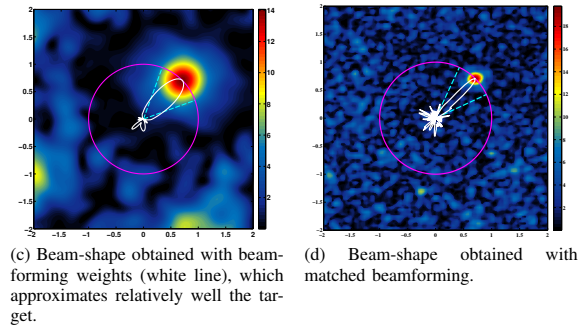


Fig. 2: Filtering a range of directions with flexibeam for  $\Theta = 40^\circ$  and 96 antennas. The beam-shape covers a much wider range of directions than matched beamforming.

which, for an arbitrary target radiation pattern, would be calculated numerically. However, the target and extended radiation pattern can be designed so that an analytical Fourier transform exists. In particular, and relevant for the example we show in the next section, the  *$n$ -dimensional symmetric Gaussian*

$$\hat{\omega}(\mathbf{r}) = \frac{1}{(2\pi)^{n/2} \sigma^n} e^{-\frac{\|\mathbf{r}-\mathbf{r}_0\|^2}{2\sigma^2}}, \quad (5)$$

with mean  $\mathbf{r}_0 \in \mathbb{S}^{n-1}$  and standard deviation  $\sigma$  has Fourier transform

$$w(\mathbf{p}) = (2\pi)^n e^{-2\pi^2 \sigma^2 \|\mathbf{p}\|^2} e^{-j2\pi\langle \mathbf{p}, \mathbf{r}_0 \rangle}. \quad (6)$$

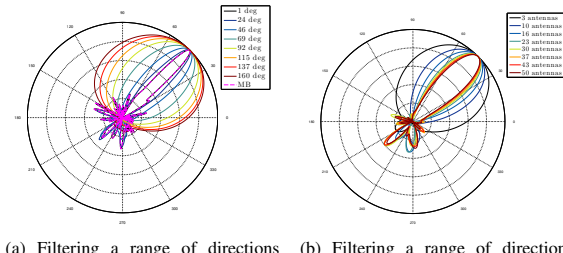
Consider now  $L$  antennas with positions  $\mathbf{p}_i$ ,  $i = 1 \dots L$ . The beamforming weight for antenna  $i$  is then

$$\frac{w(\mathbf{p}_i)}{\sqrt{\sum_{i=1}^L |w(\mathbf{p}_i)|^2}} = \frac{w(\mathbf{p}_i)}{\beta}.$$

Hence, the gains  $\gamma_i$  and phase delays  $\phi_i$  for antenna  $i$  are given by

$$\gamma_i = \frac{|w(\mathbf{p}_i)|}{\beta}, \quad \phi_i = \arg(w(\mathbf{p}_i)), \quad i = 1, \dots, L.$$

The normalisation  $\beta$  prevents antennas from having too high diversity in magnitude, which would magnify their response to channel noise.



(a) Filtering a range of directions with flexibeam for various angles and 96 antennas.  
 (b) Filtering a range of directions with flexibeam for  $\Theta = 35^\circ$  with varying number of antennas.

Fig. 3: Evolution of the flexibeam beam-shape for various angles and antennas.

How closely the beamforming achieves the target radiation filter over the sphere  $S^n$  depends strongly on the number and position of the antennas. This effectively is the ability of an FIR filter to approximate an IIR filter using a given number of taps (antennas).

### III. TRACKING WITH FLEXIBEAM

Suppose we wish to track the direction of a target moving on the plane. We initially think it is located at  $\hat{\theta}_0 = 45^\circ$ , but are uncertain. If we try to target it using too narrow a beam we could miss the target altogether. We thus calculate beamforming weights using flexibeam so as to obtain a radiation pattern with a wide enough main lobe, centred around our estimate  $\hat{\theta}_0 = 45^\circ$ . This wider beam permits tracking for a longer period of time, which avoids having to refresh the beam too often as the target moves.

From experimental conditions, the optimal radiation pattern  $\hat{w}(\theta)$  was estimated to be

$$\hat{w}(\theta) = \frac{1}{\sqrt{2\pi}\Theta} e^{-\frac{(\theta-\hat{\theta}_0)^2}{2\Theta^2}}, \quad (7)$$

where  $\theta$  is an angle on the unit circle  $S^1$  measured in degrees, and  $\Theta = 40^\circ$  is the desired width of the main lobe. For practical purposes, we propose to extend  $\hat{w}(\theta)$  to  $\mathbb{R}^2$  by the 2D symmetric Gaussian function (5), with  $r_0 = (1, 1)/\sqrt{2} \in S^1$ ,  $\sigma = \sqrt{2 - 2 \cos \Theta}$ . Strictly speaking, this is only an approximate extension of Eq. (7). However, for reasonable beam widths  $\Theta$ , this approximation is accurate enough (see Fig. 2a), and conveniently provides us with an analytical expression for the beamforming function, shown on Fig. 2b.

The beamforming weights are determined by sampling the beamforming function at the antennas' positions (see Fig. 2b). The resultant beam-shape in Fig. 2c can be seen in general to be a good approximation. In contrast, matched beamforming would require steering towards many directions to cover the same area, and hence would be more likely to miss the moving target if the refresh rate is not high enough.

For a fixed number of antennas Fig. 3a shows that for very small  $\Theta$  the beam-shape is essentially identical to the one

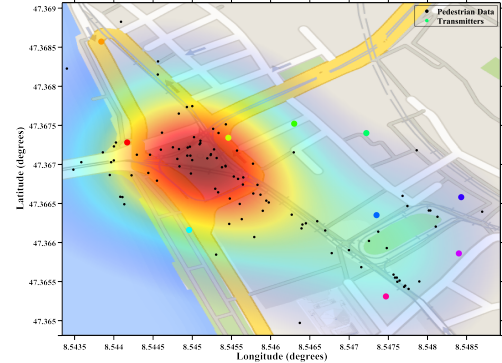


Fig. 4: Density function of pedestrians in Bellevueplatz, Zurich. The black dots are sampled positions from which the density has been inferred. The coloured dots are the transmitters.

from matched beamforming, while for larger  $\Theta$ , the beam-shape struggles to cover the whole range (because the 2D Gaussian extension does not approximate well enough the target radiation filter over the sphere). For fixed  $\Theta$ , Fig. 3b shows that the beam-shape becomes increasingly accurate as the number of antennas increases.

### IV. EXAMPLE USING MOBILE BASE STATIONS

We now illustrate an example for beamforming a collection of 3G/4G transmitters, in order to cover optimally Bellevueplatz, a portion of the city of Zurich, given probable client positions. Bellevueplatz has an approximate area of 0.08 km<sup>2</sup>, and welcomes one of the biggest tram stations with correspondingly dense pedestrian traffic. For this experiment, we gathered positions of pedestrians in this area (black dots on Fig. 4), and inferred a continuous density function (the coloured regions). This density function is called the *preference function*. It describes where the power is most needed. The goal is then to beamform from each of the 10 transmitters (the coloured dots), so that they, based on pedestrian density, jointly cover the area well.

We assume devices are in the far-field and that the channel has a narrow bandwidth. For simplicity, we neglect signal attenuation. Each transmitter has 27 antennas arranged on three concentric circles of radii 5, 15 and 25cm respectively. Moreover, they are assumed to have an emission range of approximatively 100m. Hence, each transmitter only sees a circular cut of a 100m radius of the density function, which defines the individual transmitter preference function  $f_i \in \mathcal{L}^2(\mathbb{R}^2)$ ,  $i = 1, \dots, 10$ .

The beam determination problem for each transmitter consists then of four steps:

- 1) Compute the target radiation pattern by taking the radial projection of the individual preference functions from

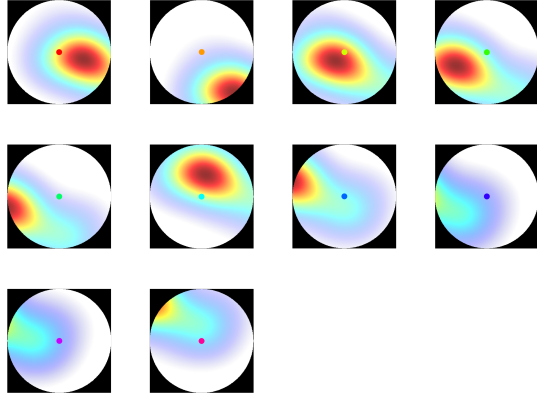


Fig. 5: Circular cuts of the density function in Fig. 4 based on the range of each transmitter.

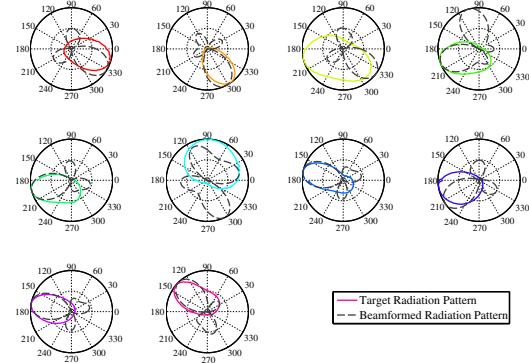
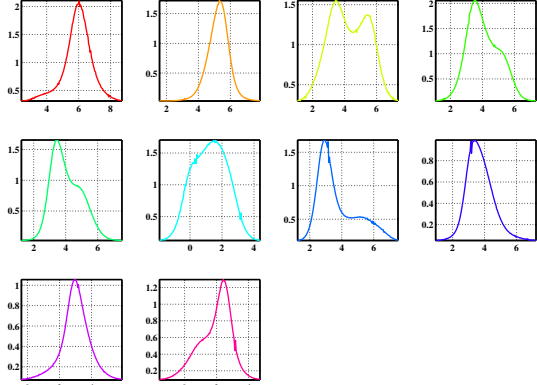
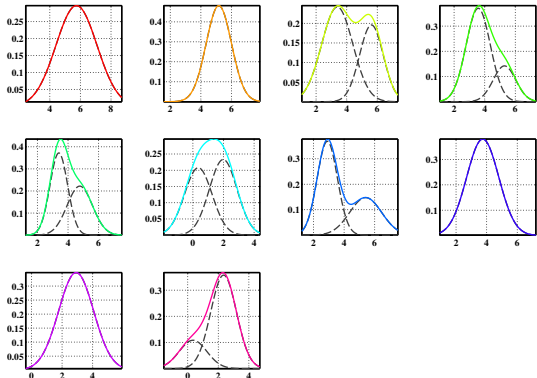


Fig. 7: Comparison between the target radiation pattern (coloured lines) and the actual achieved beam-shape (dashed grey lines) for each transmitter.



(a) Target radiation patterns for each transmitter plotted over a segment of length  $2\pi$ .



(b) Approximation of the target radiation patterns by a sum of weighted Gaussian functions.

Fig. 6: Target radiation patterns for each transmitter and their approximation by a sum of weighted Gaussian functions.

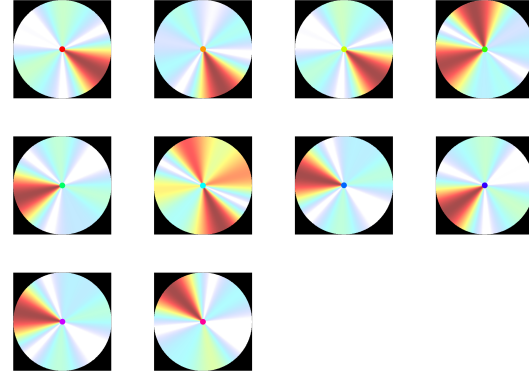


Fig. 8: The transmitters cover more areas with a high density of pedestrian (compare with Fig. 5).

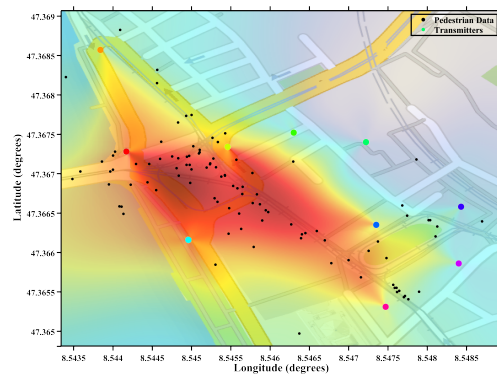


Fig. 9: The summation of the beam-shapes from each transmitter gives the joint coverage. Joint coverage achieved by all the transmitters after choosing the beamforming weights. Areas with high pedestrian density are better covered.

Fig. 5,

$$\hat{w}_i(\theta) = \int_0^{100} f_i(r \cos \theta, r \sin \theta) dr,$$

with  $\theta \in [0, 2\pi]$ .

- 2) Approximate this target filter by a sum of weighted Gaussian functions (see Fig. 6b),

$$\hat{w}_i(\theta) \simeq \sum_{k=1}^{N_i} \frac{\alpha_k^{(i)}}{\sqrt{2\pi}\Theta_k^{(i)}} e^{-\frac{(\theta - \mu_k^{(i)})^2}{2\Theta_k^{(i)}2}},$$

where  $N_i \in \mathbb{N}$ ,  $\alpha_k^{(i)}, \Theta_k^{(i)} > 0$  and  $\mu_k^{(i)} \in [0, 2\pi]$  are respectively the least squares estimates of the number of Gaussian components and their associated weights, standard deviations and means.

- 3) Extend this filter to the plane with the same technique as described in Section III and compute its Fourier transform analytically using Eq. (6). We get

$$\hat{\omega}_i(x, y) = \sum_{i=1}^{N_i} \alpha_k^{(i)} \Phi \left( \frac{x - \cos(\mu_k^{(i)})}{\sigma_k^{(i)}}, \frac{y - \sin(\mu_k^{(i)})}{\sigma_k^{(i)}} \right),$$

where  $(x, y) \in \mathbb{R}^2$ ,  $\Phi \in \mathcal{L}^2(\mathbb{R}^2)$  is the standard 2D Gaussian function and  $\sigma_k^{(i)} = \sqrt{2 - 2 \cos(\Theta_k^{(i)})}$ .

- 4) Compute the weights to be applied to each antenna composing the transmitter by sampling the Fourier transform at the locations of the antennas.

Most of the transmitter beam-shapes, shown in Fig. 7, approximate the associated target filter well, despite unavoidable side-lobes due to the finite number of antennas. Fig. 9 shows that areas with higher pedestrian density are better covered than before, giving them better signal, as less power is dissipated in unnecessary areas.

## V. CONCLUSIONS

We took the flexibeam technique to determine beamforming weights for a target spatial filter, and explained it from the transmit beamforming perspective. We then showed on an example how it can be used by groups of mobile base stations to concentrate energy where devices are concentrated.

We argued the case for targeting regions rather than single points, and showed that this could be achieved. One interesting effect is that the MIMO optimisation tradeoff between (focused) beamforming and spatial diversity (multiple replicas of the radio signal from different directions) [10] can be circumvented.

Of course in practise real-life data transfer and the resultant communications protocol is far more complicated, and beamforming is just one component in the mix. Future work includes incorporating these together, and adding cooperation between the stations to maximise throughput and minimise latency.

## REFERENCES

- [1] R.-T. Juang, K.-P. Yar, K.-Y. Lin, and P. Ting, "Decentralized multiuser beamforming for cellular communication systems," in *Wireless and Mobile Computing, Networking and Communications (WiMob), 2011 IEEE 7th International Conference on*, Oct 2011, pp. 260–264.
- [2] C. Jiang and L. Cimini, "Energy-efficient multiuser mimo beamforming," in *Information Sciences and Systems (CISS), 2011 45th Annual Conference on*, March 2011, pp. 1–5.
- [3] J. Jin, C. Lin, Q. Wang, H. Yang, and Y. Wang, "Effect of imperfect channel estimation on multi-user beamforming in lte-advanced system," in *Vehicular Technology Conference (VTC 2010-Spring), 2010 IEEE 71st*, May 2010, pp. 1–5.
- [4] D. H. Johnson and D. E. Dodgeon, *Array signal processing: concepts and techniques*. Simon & Schuster, 1992.
- [5] B. D. Veen and K. M. Buckley, "Beamforming: a versatile approach to spatial filtering," *ASSP Magazine, IEEE*, vol. 5, no. 2, pp. 4–24, 4 1988.
- [6] Y.-S. Cheng and C.-H. Chen, "A novel 3d beamforming scheme for lte-advanced system," in *Network Operations and Management Symposium (APNOMS), 2014 16th Asia-Pacific*, Sept 2014, pp. 1–6.
- [7] P. Hurley and M. Simeoni, "Flexibeam: analytic spatial filtering by beamforming," in *International Conference on Acoustics, Speech and Signal Processing (ICASSP), IEEE*, March 2016 (to appear).
- [8] R. J. Mailloux, "Phased array antenna handbook," *Boston, MA: Artech House, 1994*, 1994.
- [9] W.-Q. Wang and H. Shao, "A flexible phased-mimo array antenna with transmit beamforming," *International Journal of Antennas and Propagation*, vol. 2012, 2012.
- [10] A. Sibile, C. Oestges, and A. Zanella, *MIMO: from theory to implementation*. Academic Press, 2010.